

SUPPLEMENTAL INFORMATION

INVENTORY

Supplementary Methods

Supplementary Figure Legends

Supplementary References

Supplementary Figures 1-10

SUPPLEMENTARY METHODS

Oral administration of CA. Administration of single doses of CA (dissolved in B.P. compliant olive oil) to C57BL/6J mice by gavage, and preparation of lysates from isolated intestinal epithelia were done essentially as previously described (1). Briefly, dissected small intestines (from stomach to caecum) were opened longitudinally, minced into 2-3 mm pieces at 5°C, washed for 10 minutes in ice-cold phosphate-buffered saline (PBS) plus 1 mM DTT, and subsequently dissociated by successive incubations (at 5°C, for 10 minutes each) in 10 ml PBS containing 10 mM EDTA under vigorous shaking. Supernatant fractions (typically from 4-5 incubations) were collected until no further cells were released, and combined. Samples were further processed for protein and RNA extraction using the RNeasy mini kit (Qiagen) if epithelial purity was judged to be >95% (based on flow cytometry after α -EpCam staining).

SUPPLEMENTARY FIGURE LEGENDS

Suppl. Fig. 1

Molecular targets of β -catenin inhibitors

Schematic representation of the Wnt signaling pathway, with positive (green) and negative (red) components (salmon underlay, Axin degradasome). Axin promotes the phosphorylation of ABC by scaffolding GSK3 and CK1 α , thereby generating PBC, which is targeted for

proteasomal degradation. Tankyrase (TNKS) destabilizes Axin, by poly(ADP)ribosylating it and targeting it for ubiquitylation and subsequent proteasomal degradation. Its inhibition by IWR-1 (2) and XAV939 (3) results in Axin stabilization, and in destabilization of β -catenin. Similarly, pyrvinium (an agonist of CK1 α) promotes phosphorylation of ABC, and degradation of β -catenin (4). ICG-001 inhibits β -catenin's binding to CBP (5), whereas PKF115-584 (6) and iCRT3 (7) inhibit its binding of TCF. CA acts through an intrinsically unstructured α -helix in the N-terminus of β -catenin, blocking its binding to BCL9/B9L and promoting its aggregation and proteasomal degradation (8). The molecular target of 16k is unknown (9).

Suppl. Fig. 2

Efficacy and toxicity of β -catenin inhibitors

(A) Cell lines used for inhibitor assays (based on TCF-dependent reporters), and IC₅₀ values (first two columns, as determined in this study; last column, as previously determined (see **suppl. Fig. 1** for references); n/a, no inhibition; n/d, not determined (due to high toxicity, see C). (B) SuperTOP assays from HEK293T cells (○), simultaneously exposed to Wnt3a-conditioned medium (WCM) and to inhibitors at the indicated concentrations, or from inhibitor-treated SW480 cells (●); values are shown as % of mock-treated controls. (C) Cell toxicity assays of HEK293T (○) and SW480 cells (●); the numbers of inhibitor-treated cells were quantified relative to mock-treated controls (100%) after 24 hours of treatment at the indicated concentrations, as previously described (8). Treatment of HEK293T and SW480 cells with 5 μ M PKF115-584 (6) resulted in >80% toxicity after 24 hours.

Suppl. Fig. 3

Effects of TNKSi on Wnt signaling components

(A) SuperTOP assays in SW480 cells, following incubation with increasing concentrations of XAV939 (as indicated above panel) with (■) or without (●) 25 μ M CA, or with increasing

concentrations of CA (as indicated below panel) with (■) or without (●) 2.5 μ M XAV939 for 24 hours; relative activities are shown as % of mock-treated controls. (B) SuperTOP assays of DLD-1 cells, treated with increasing concentrations of XAV939 (■, concentrations above panel) or CA (●, concentrations below panel) for 24 hours (IC_{50} , 0.7 μ M); relative activities are shown as in A). (C) Western blots from XAV939-treated cells (as indicated above panel), probed with antibodies as indicated.

Suppl. Fig. 4

TNKS*i*-induced Axin degradasomes

(A, B) Single confocal sections through SW480 cells treated with 2.5 μ M XAV939 for 24 hours, fixed and co-stained with antibodies as indicated in panels. (A) Axin degradasomes are positive for ABC, but negative for CtBP (see (10)), phospho-LRP6, and poly(ADP-ribose) (PAR). (B) Axin degradasomes (blue in merges; top, labelled by α -TNKS; bottom, labelled by α -AXIN1) neither co-localize with p62-positive autophagosomes (red in merge, top) nor with EEA1-positive endosomes (red in merge, bottom). (C-E) Single confocal sections through (C) HEK293T, (D) HCT-116 or (E) HeLa cells, treated with 2.5 μ M XAV939 for 24 hours, fixed and co-stained with antibodies against β -catenin, AXIN1 and TNKS as indicated in panels. Size bars, 10 μ M.

Suppl. Fig. 5

TNKS*i* treatment of COLO320 cells

SW480 and COLO320 cells, inhibitor-treated as indicated; (A) Western blots of lysates, probed with antibodies as indicated; (B) Single confocal sections through *APC*-mutant colorectal cancer cells, as indicated; merges show magnifications from boxed areas (red, APC; green, AXIN1). Size bars, 10 μ M.

Suppl. Fig. 6

Prolonged TNKSi treatment and β -catenin stability

(A) Western blots of lysates from SW480 cells, XAV939-treated for 1-5 days, probed with antibodies as indicated. (B) FACS analysis of SW480 cells stably transfected with TOP-GFP, treated as indicated on the right. (C) qRT-PCR analysis of transcripts from SW480 cells after 1-5 days of inhibitor treatment; expression levels of genes indicated above panel are relative to *TBP* (internal control). Statistical significance $P < 0.01$ (*) or < 0.001 (**). (D) Single confocal sections through SW480 cells treated with 2.5 μ M XAV939 for 1-5 days as indicated, fixed and co-stained with antibodies against AXIN1 and β -catenin; size bars, 10 μ M. (E) Western blots probed for β -catenin in detergent-soluble (cytoplasmic) and detergent-insoluble (nuclei-enriched) fractions of cycloheximide-treated SW480 cells (collected by centrifugation at 800 *g*, after incubation in 0.1 mg/ml cycloheximide), and subsequent lysis in 20 mM HEPES (pH 7.9, containing Roche protease inhibitor cocktail), 400 mM NaCl, 1 mM EDTA, 25% glycerol at the indicated time points. *Underneath*, densitometry of Western blots, showing ratios of detergent-insoluble β -catenin relative to detergent-soluble β -catenin ($t_{1/2}$ of detergent-insoluble β -catenin, ~ 1 hour).

Suppl. Fig. 7

TNKSi of chronically Wnt-stimulated HeLa cells

SuperTOP assays of HeLa cells treated with XAV939 as in main **Fig. 3A**; shown are relative activities (in %) of WCM-treated controls (dotted line).

Suppl. Fig. 8

TNKSi responses of Wnt-stimulated cells

(A-C) SuperTOP assays in HEK293T cells, transfected for 24 hours to express proteins indicated below panels, followed by (A) mock treatment, (B) treatment for 24 hours with WCM or (C) Wnt pre-treatment as in main **Fig. 3A**; shown are relative activities (in %) of WCM-treated controls (dotted lines in A and C), or total values (B); statistical significance P

< 0.01 (*) or < 0.001 (**). **(D)** Western blot of lysates from HEK293T cells, probed with antibodies as indicated, after treatment for 24 hours with control siRNA, or with siRNAs against B9L or LEF1, followed by incubation with control or WCM for 6 hours, followed by mock-treatment or treatment with 2.5 μ M XAV939 for 24 hours, as indicated above.

Suppl. Fig. 9

CA treatment of mice

(A) Flow cytometry analysis of total lysates from isolated epithelia, prepared from dissected small intestines of *C57BL/6J* mice (following oral administration of a single dose of CA, as in main **Fig. 6B**). A sample was discarded if the EpCam-positive fraction (dark profile) was <95% (in 3/44 experimental mice); grey profile, isotype control. **(B)** Western blots of intestinal lysates from 3 independent experiments (expt I – III, each with cohorts of 4-5 mice), generated from dissected small intestines harvested at various time points after a single oral CA dose (as indicated above panels), probed with antibodies as indicated next to panels (note that the exposures are comparable within, but not between, different experiments); 50 μ g of protein were loaded per lane. Each lane corresponds to one experimental animal from which a successful lysate was obtained (n=41, see **A**); β -catenin signals were quantified by densitometry, and values were calculated relative to each corresponding mock-treated control, and shown as single data points in main **Fig. 6B**. **(C)** Diameters of intestinal tumors of 105 day old *Apc^{Min}/+* mice (n=9 in each cohort), after dietary supplementation of CA (0.1% or 1%) or carnosol (CO) (0.1%); *P* values (from *t* tests) are relative to controls. For histological examination of CA-treated and control tumors, methacarn- or formalin-fixed intestines were rolled up ('swiss rolls') following tumor scoring, and processed as described (1), but there were no detectable differences in overall morphology of intestinal crypts or villi from control and treatment groups, nor in gross rates of proliferation and apoptosis, nor in the levels of specific markers (c-myc, Axin2, nuclear β -catenin) between the tumors from the different groups.

Suppl. Fig. 10

Comparison of LEF1 antibodies

Left, single confocal section through a carcinoma tissue core, co-stained with antibodies against β -catenin (red), LEF1 (C18A7, green; C12A5, far red) and DAPI (blue); the exposure of the top-left panel was increased to reveal background staining by C12A5 (an antiserum from Cell Signaling, previously used by (11)). *Right*, single confocal section of signet ring-cell carcinoma, co-stained for β -catenin (red), LEF1 (C18A7, green) and DAPI (blue), showing characteristic peripheral nuclei displaced by mucinous vacuoles which are negative for β -catenin and LEF1 staining. Size bars, 25 μ M.

SUPPLEMENTARY REFERENCES

1. Metcalfe C, Ibrahim AE, Graeb M, de la Roche M, Schwarz-Romond T, Fiedler M, et al. Dvl2 promotes intestinal length and neoplasia in the ApcMin mouse model for colorectal cancer. *Cancer Res.* 2010;70:6629-6638.
2. Chen B, Dodge ME, Tang W, Lu J, Ma Z, Fan CW, et al. Small molecule-mediated disruption of Wnt-dependent signaling in tissue regeneration and cancer. *Nat Chem Biol* 2009;5:100-107.
3. Huang SM, Mishina YM, Liu S, Cheung A, Stegmeier F, Michaud GA, et al. Tankyrase inhibition stabilizes axin and antagonizes Wnt signalling. *Nature.* 2009;461:614-620.
4. Thorne CA, Hanson AJ, Schneider J, Tahinci E, Orton D, Cselenyi CS, et al. Small-molecule inhibition of Wnt signaling through activation of casein kinase 1alpha. *Nat Chem Biol* 2010;6:829-836.
5. Eguchi M, Nguyen C, Lee SC, Kahn M. ICG-001, a novel small molecule regulator of TCF/beta-catenin transcription. *Med Chem* 2005;1:467-472.

6. Lepourcelet M, Chen YN, France DS, Wang H, Crews P, Petersen F, et al. Small-molecule antagonists of the oncogenic Tcf/beta-catenin protein complex. *Cancer Cell* 2004;5:91-102.
7. Gonsalves FC, Klein K, Carson BB, Katz S, Ekas LA, Evans S, et al. An RNAi-based chemical genetic screen identifies three small-molecule inhibitors of the Wnt/wingless signaling pathway. *Proc Natl Acad Sci USA* 2011;108:5954-5963.
8. de la Roche M, Rutherford TJ, Gupta D, Veprintsev DB, Saxty B, Freund SM, et al. An intrinsically labile alpha-helix abutting the BCL9-binding site of beta-catenin is required for its inhibition by carnosic acid. *Nat Commun* 2012;3:680.
9. Chen Z, Venkatesan AM, Dehnhardt CM, Dos Santos O, Delos Santos E, Ayralkaloustian S, et al. 2,4-Diamino-quinazolines as inhibitors of beta-catenin/Tcf-4 pathway: Potential treatment for colorectal cancer. *Bioorg Med Chem Lett* 2009;19:4980-4983.
10. Schneikert J, Brauburger K, Behrens J. APC mutations in colorectal tumours from FAP patients are selected for CtBP-mediated oligomerization of truncated APC. *Hum Mol Genet* 2011;20:3554-3564.
11. Kriegl L, Horst D, Reiche JA, Engel J, Kirchner T, Jung A. LEF-1 and TCF4 expression correlate inversely with survival in colorectal cancer. *J Transl Med* 2010;8:123.

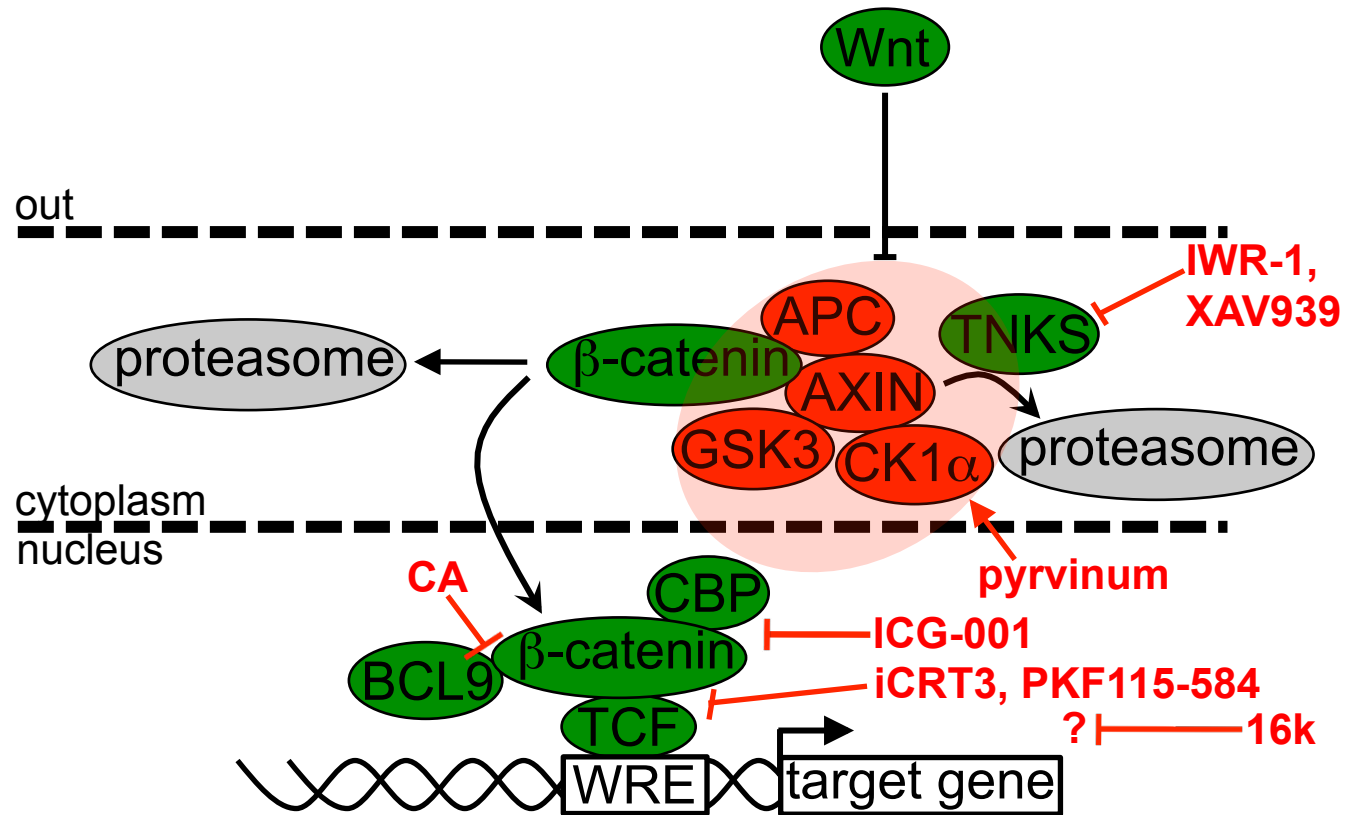


Fig. S1 de la Roche et al.

A

compound	IC ₅₀		IC ₅₀ , cell line(s)
	HEK293T	SW480	
CA	7.0 μM	13 μM	ditto
ICG-001	4.2 μM	12 μM	3 μM, SW480
XAV939	0.3 μM	n/a	0.1 μM, HEK293, SW480
IWR-1	0.1 μM	n/a	0.2 μM, L cells
16k	n/a	n/a	0.2 μM, SW480
pyrvinium	60 nM	n/a	10 nM, SW480
iCRT3	7.0 μM	n/a	8.2 nM, HEK293
PKF115-584	n/d	n/d	0.4 μM, HCT116

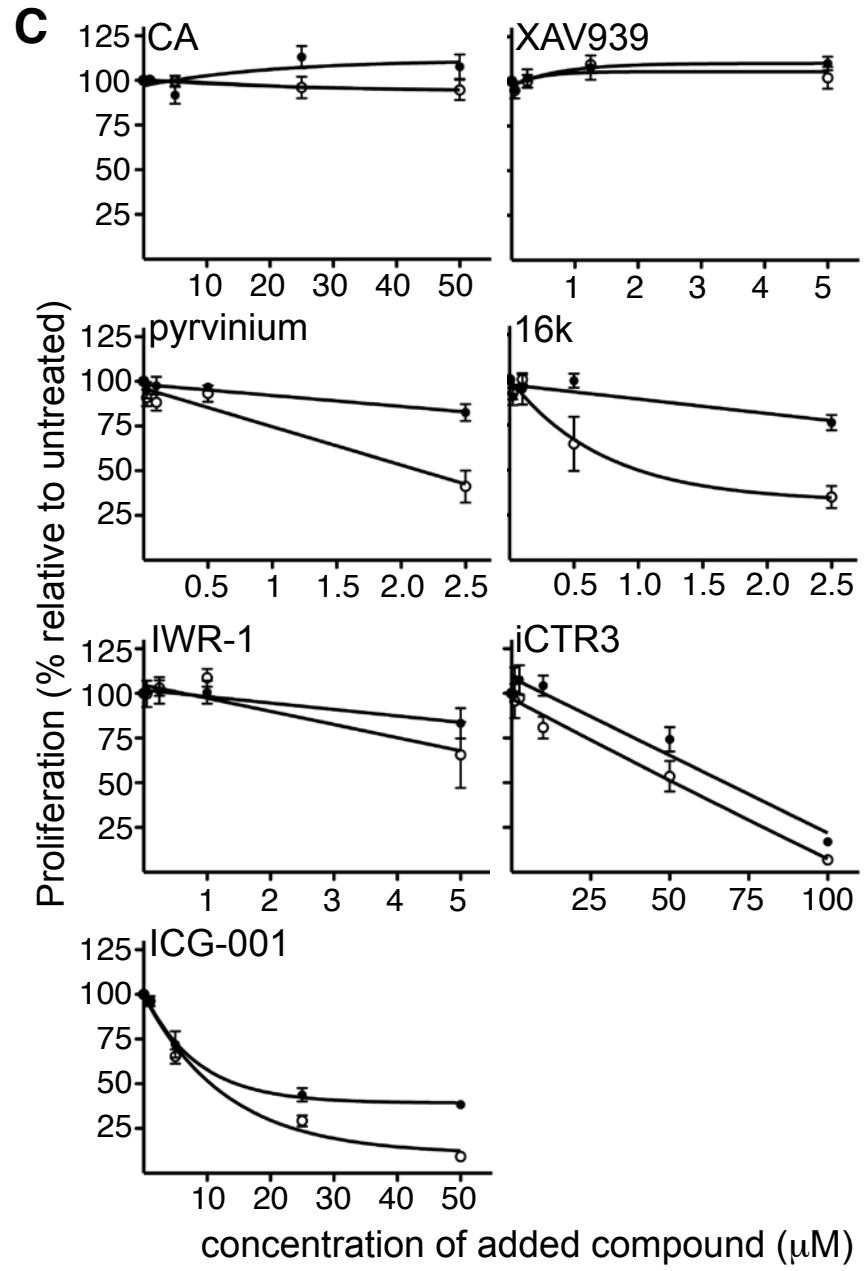
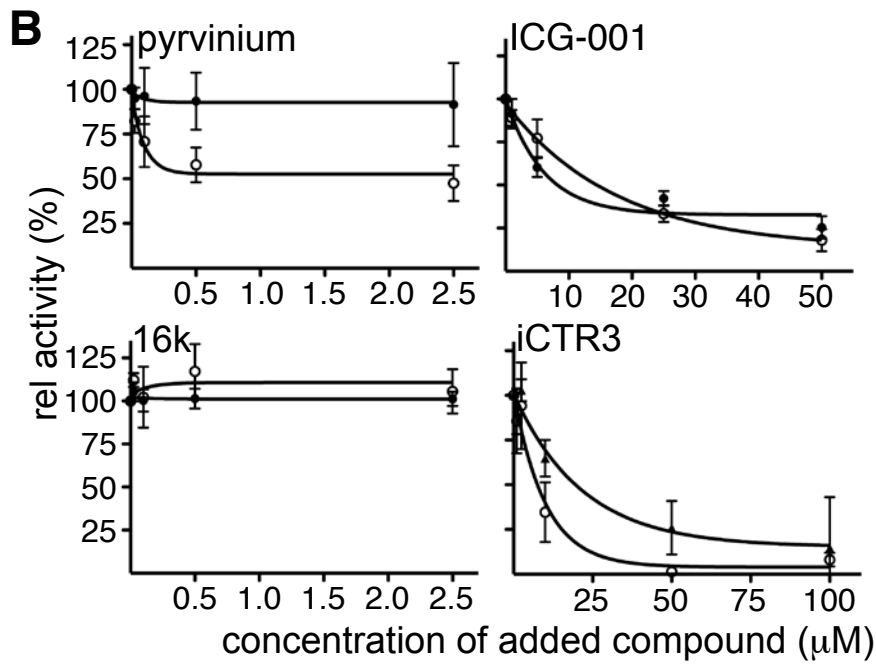


Fig. S2 de la Roche et al.

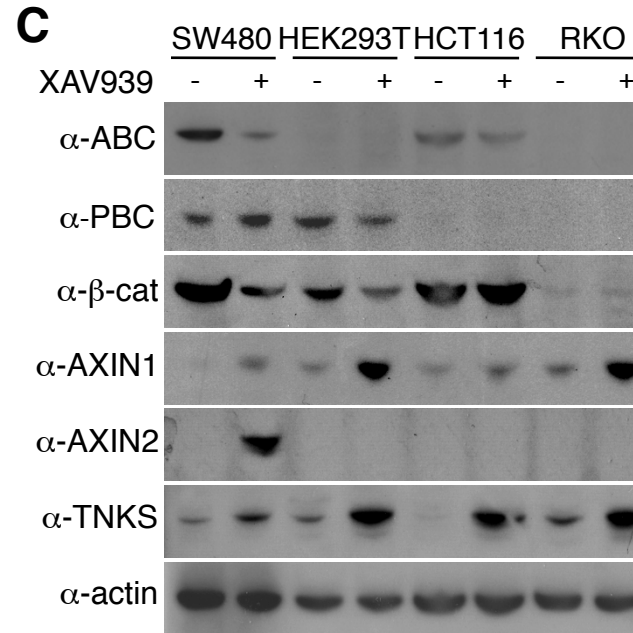
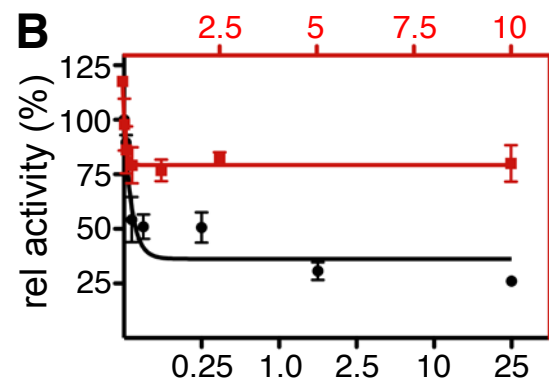
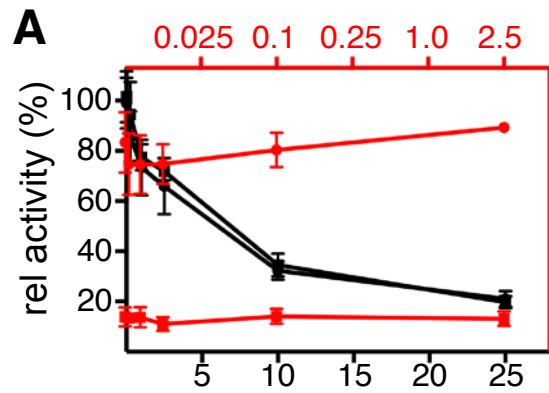


Fig. S3 de la Roche et al.

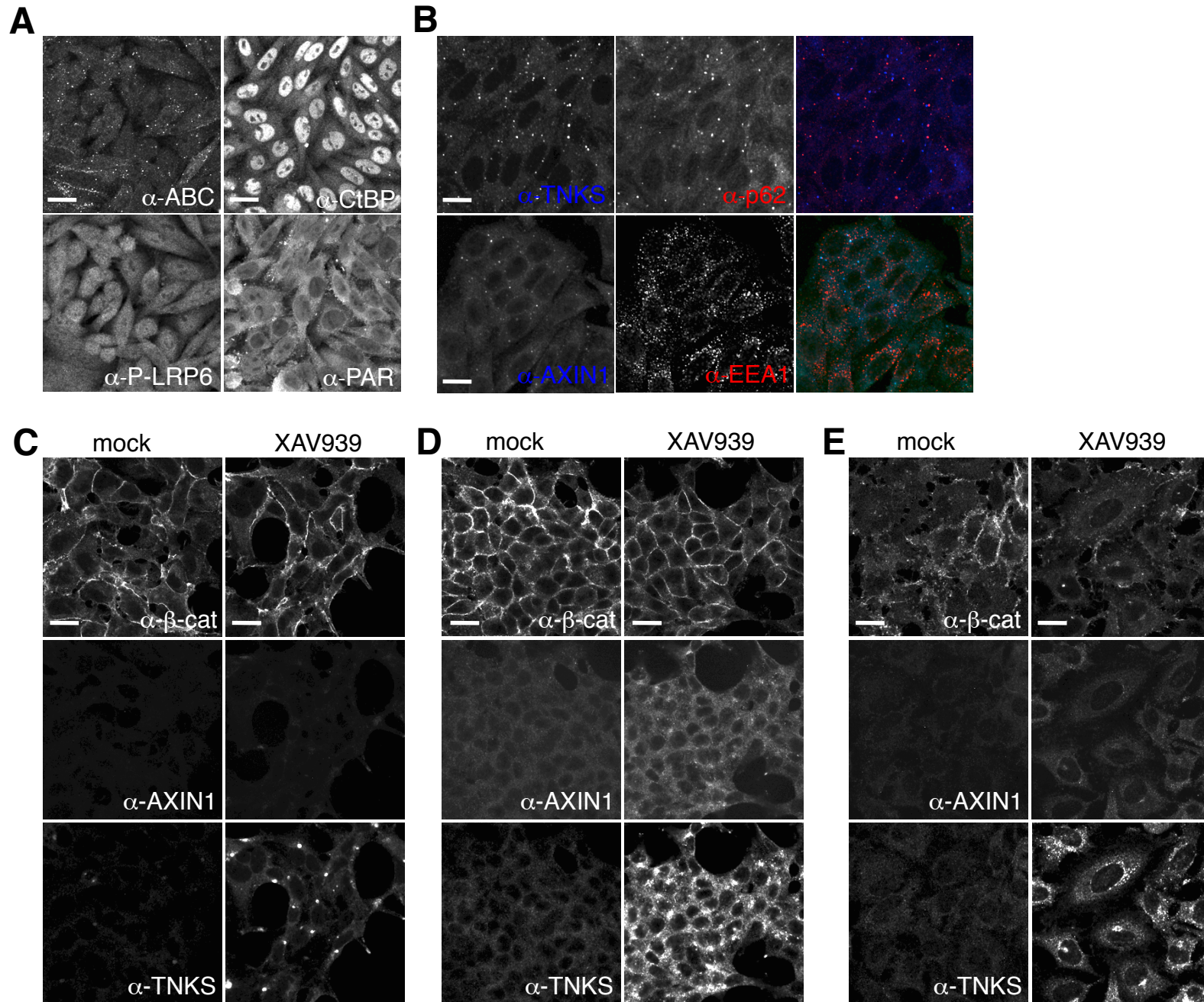


Fig. S4 de la Roche et al.

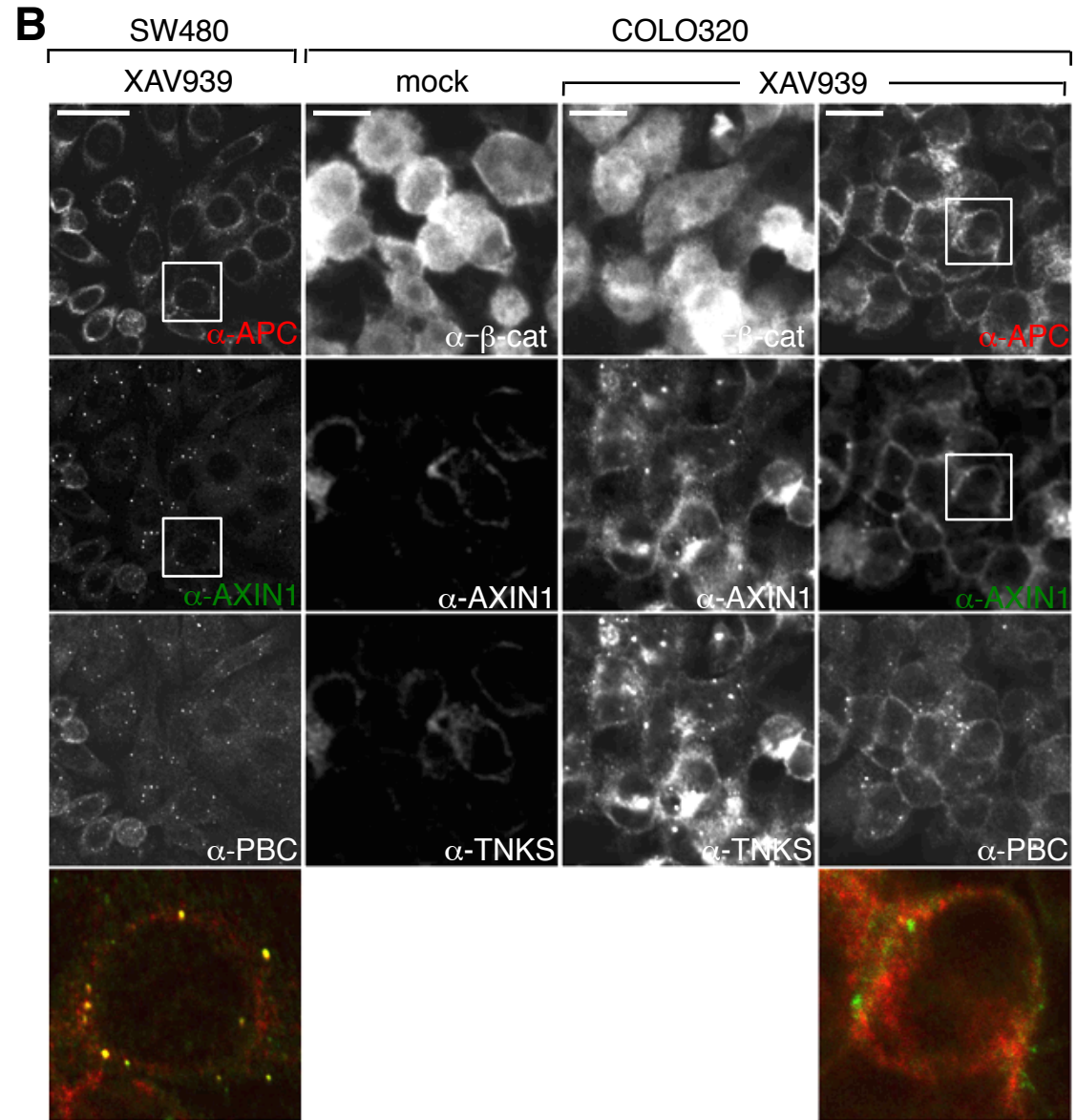
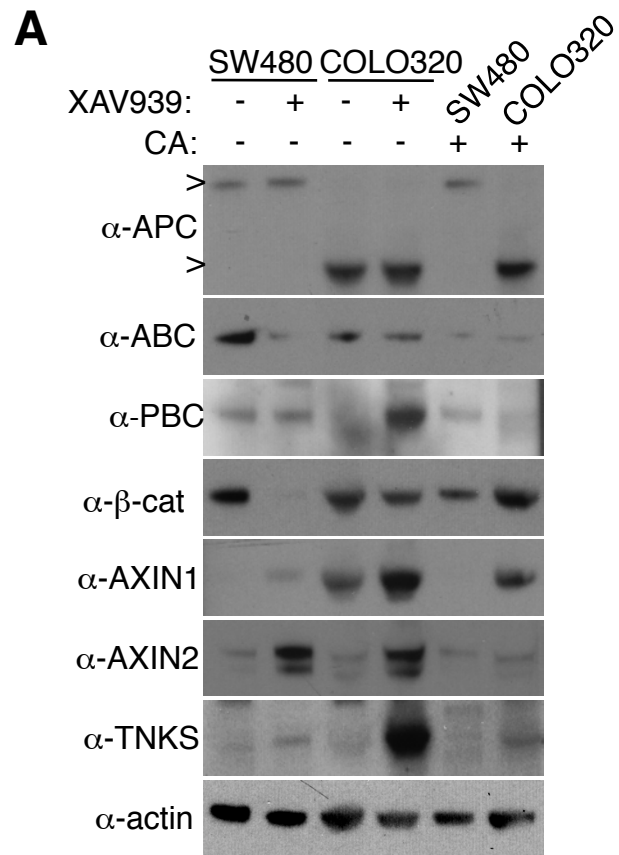


Fig. S5 de la Roche et al.

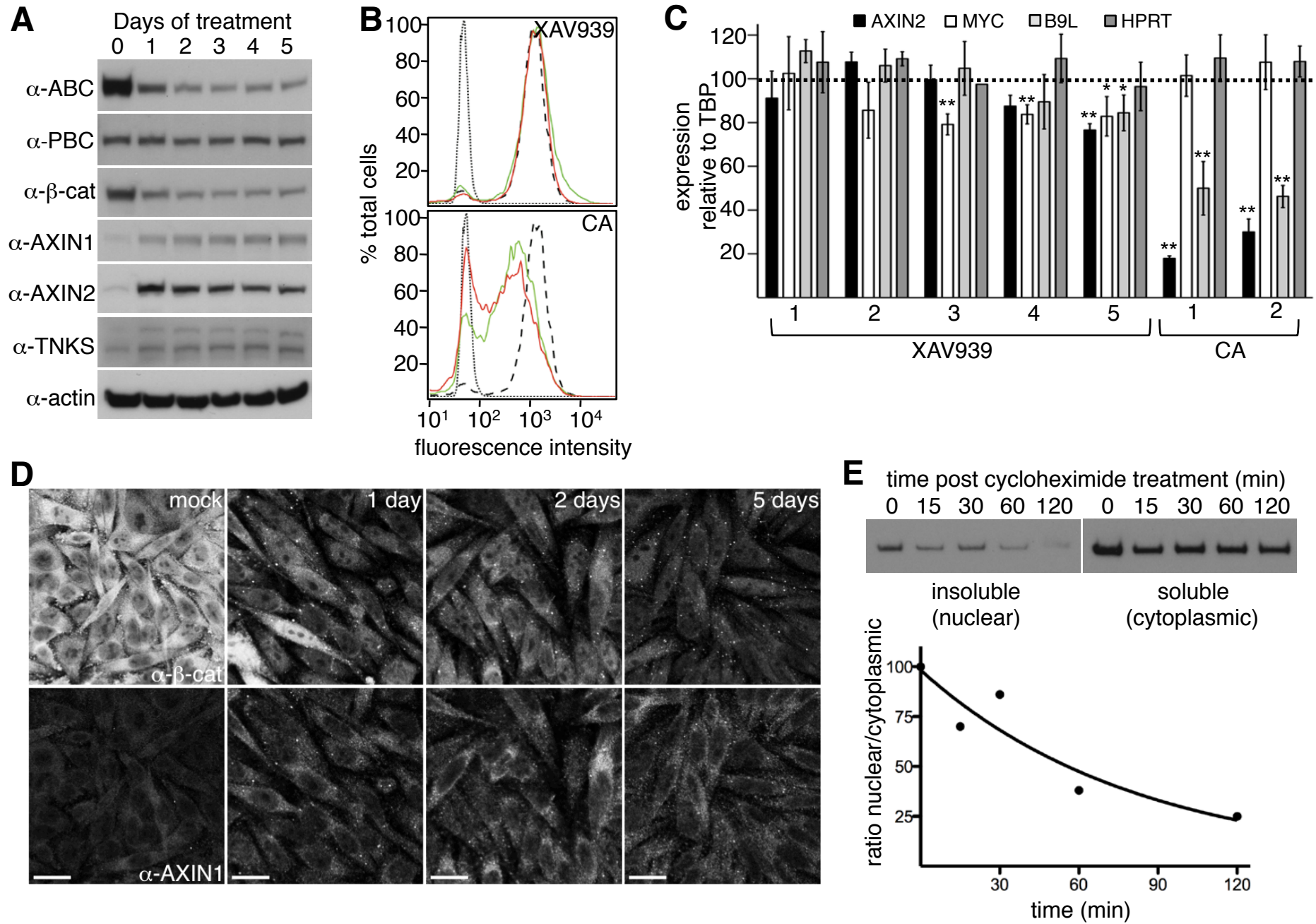


Fig. S6 de la Roche et al.

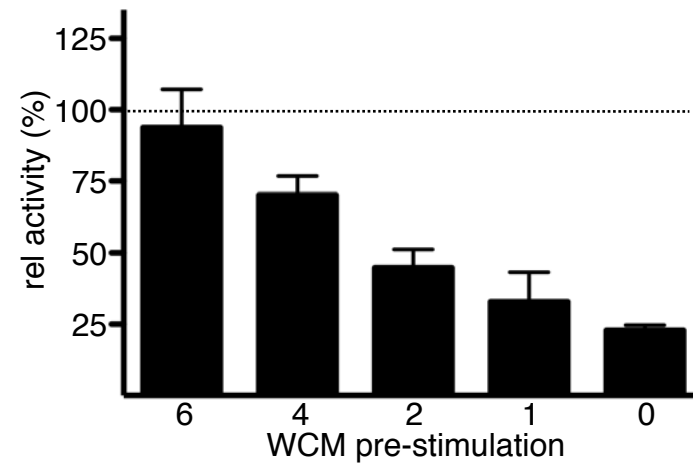


Fig. S7 de la Roche et al.

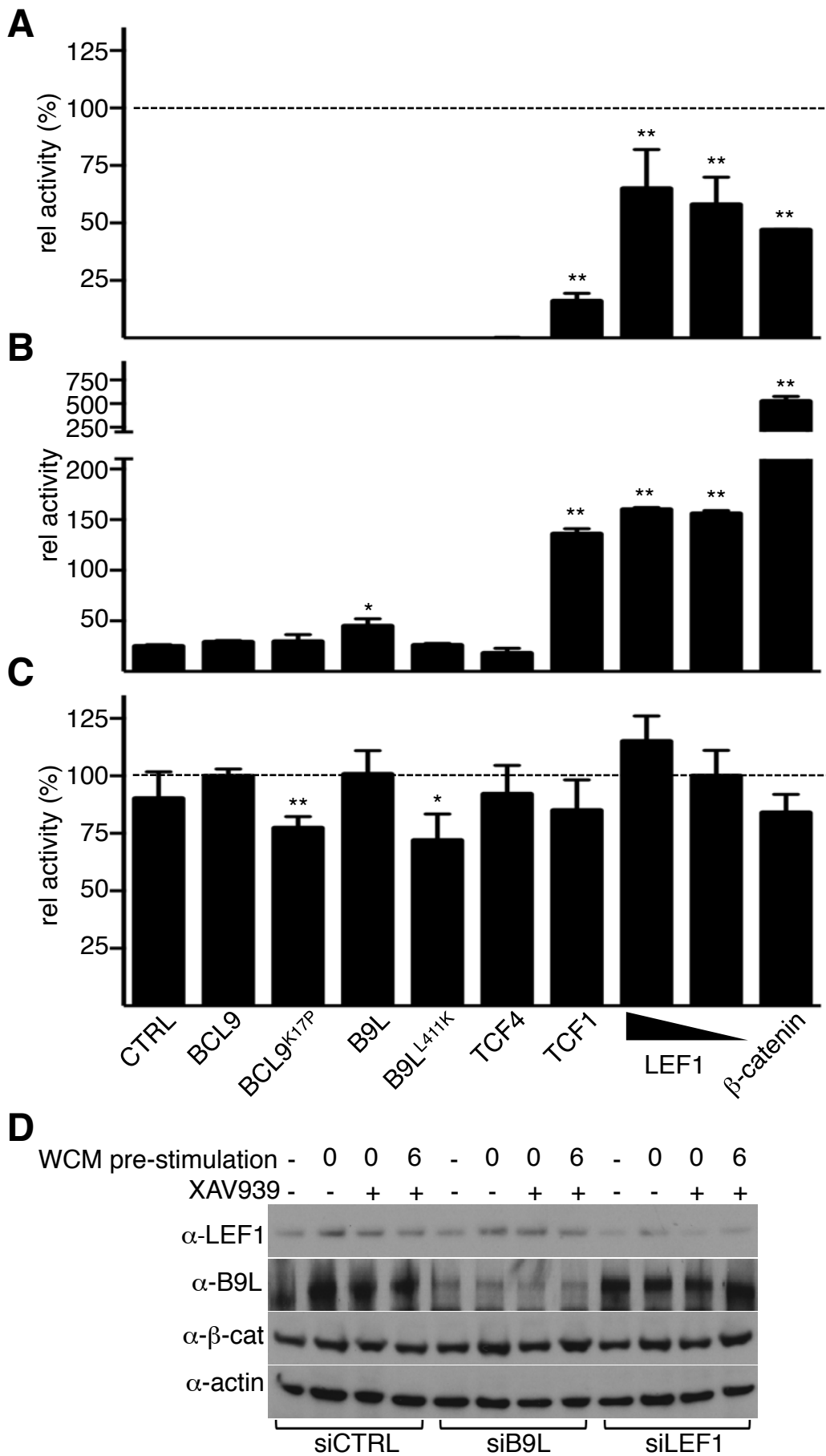


Fig. S8 de la Roche et al.

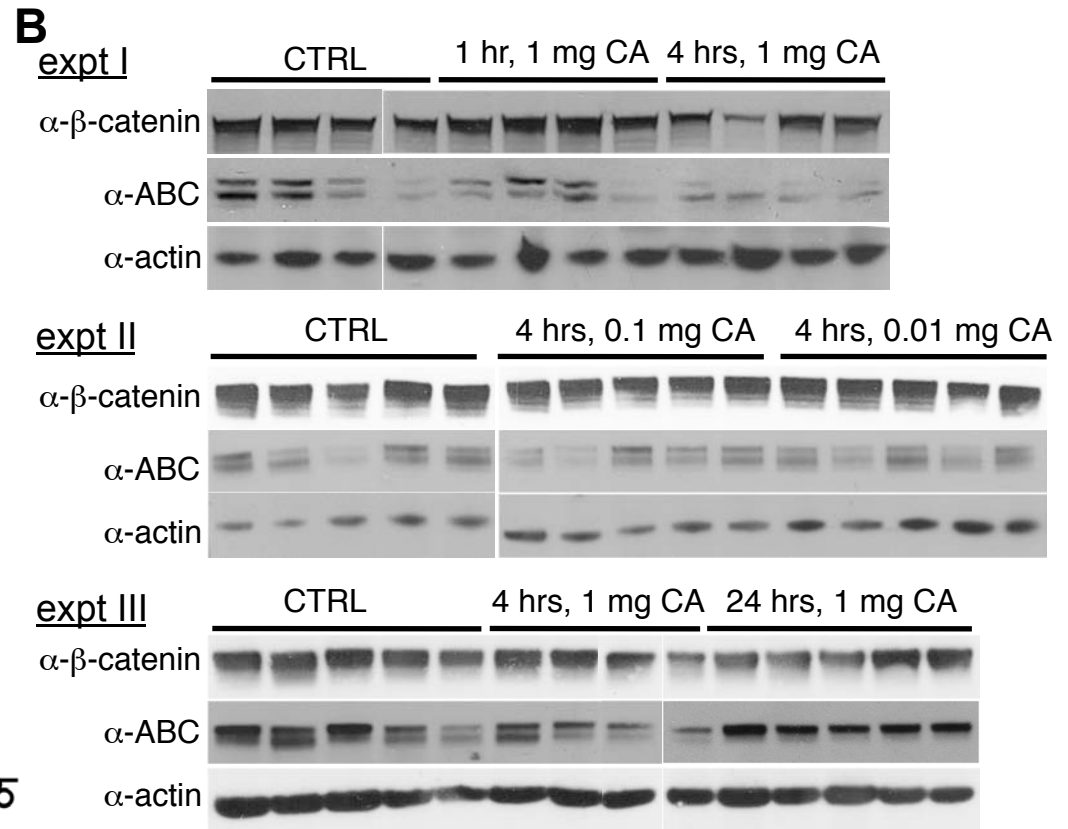
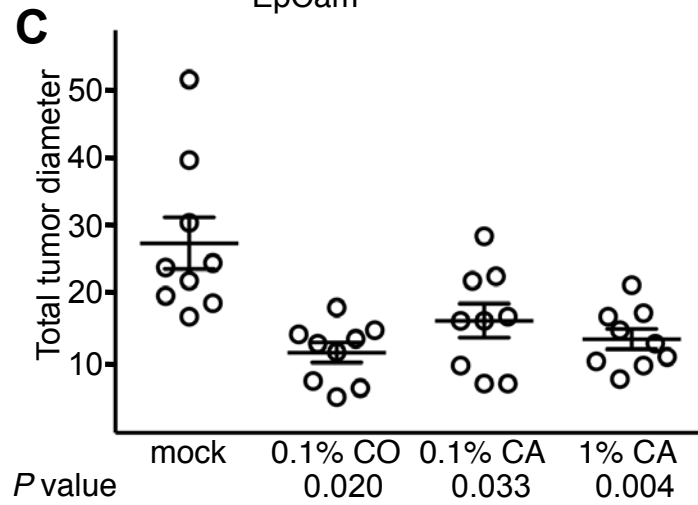
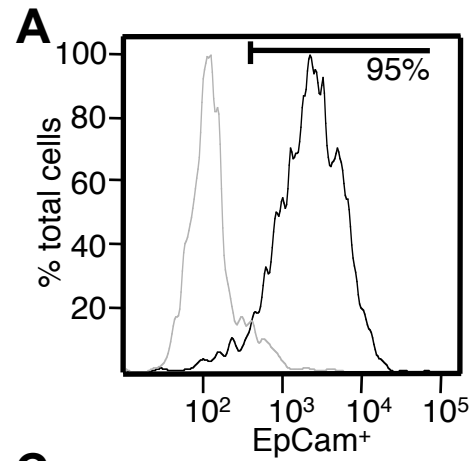


Fig. S9 de la Roche et al.

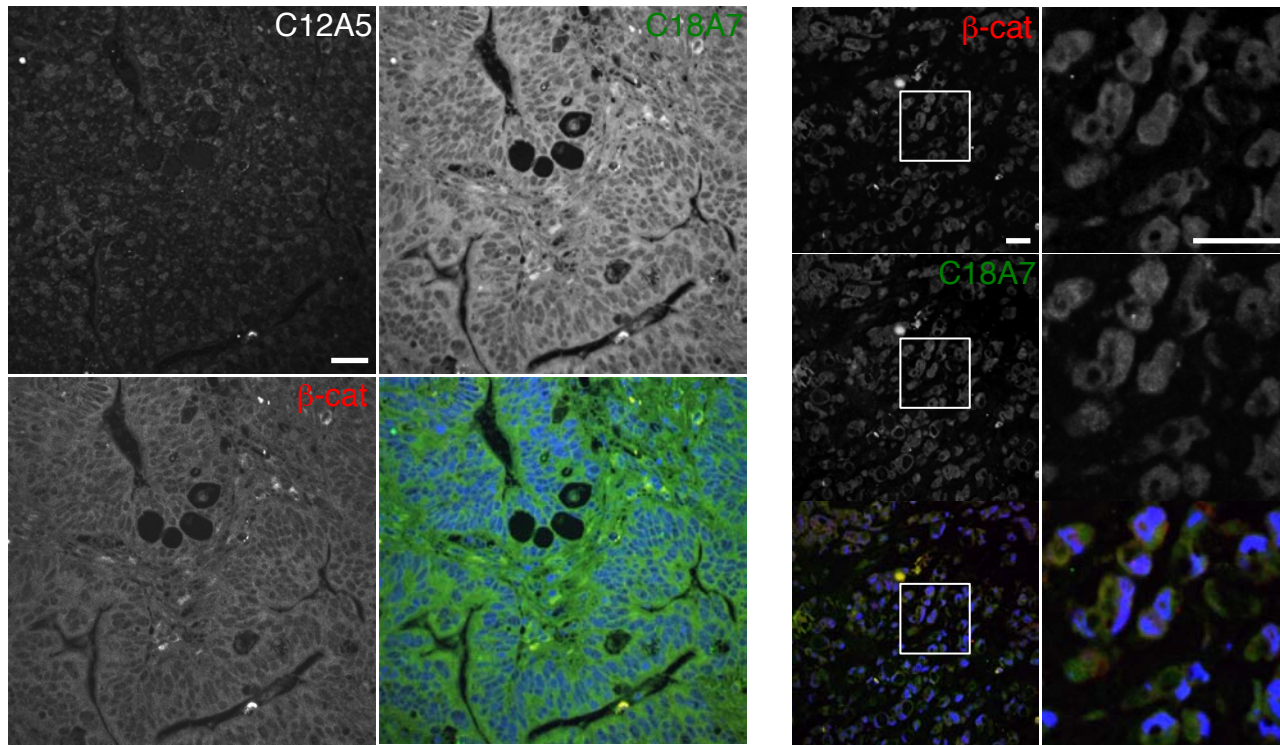


Fig. S10 de la Roche et al.